Enhanced field-driven domain-wall motion in Pt/$Co_{68}B_{32}$/Pt strips

R. Lavrijsen,[1,a)] M. A. Verheijen,[2] B. Barcones,[1] J. T. Kohlhepp,[1] H. J. M. Swagten,[1] and B. Koopmans[1]

[1]*Department of Applied Physics, Center for NanoMaterials and COBRA Research Institute, Eindhoven University of Technology, P.O. Box 513, 5600 MB Eindhoven, The Netherlands*

[2]*MiPlaza Technology Laboratories, Philips Research Europe, High Tech Campus 29, 5656 AE Eindhoven, The Netherlands*

(Received 15 February 2011; accepted 5 March 2011; published online 28 March 2011)

It is now commonly accepted that materials exhibiting high perpendicular magnetic anisotropy are excellent candidates for devices based on current-induced domain-wall (DW) motion. A major hindrance of these materials however, is that they exhibit strong DW pinning. Here we report a significant increase in the field-driven DW velocity in Pt(4 nm)/$Co_{68}B_{32}$(0.6 nm)/Pt(2 nm) layers patterned into 900 nm wide strips. We compare the DW velocity between Co and $Co_{68}B_{32}$ films and discuss the observed effects using the morphology of the films investigated by high-resolution transmission electron microscopy. © *2011 American Institute of Physics*. [doi:10.1063/1.3571548]

Magnetic domain-walls (DWs) in magnetic nanowires have attracted much attention due to their potential application in field- and current-induced DW logic and magnetic memory devices.[1,2] More recently, the attention is shifting to materials with high perpendicular magnetic anisotropy (PMA) resulting in an out-of-plane easy-axis. This high PMA results in narrow, robust, and simple Bloch DWs for which current-induced DW motion/depinning is predicted to be efficient.[3–8] Moreover, the PMA in these systems can be easily tuned by using focused Ga (Ref. 9) or He (Ref. 10) irradiation which will greatly facilitate the experiments. Fundamentally, these systems are very interesting since the recently observed Rashba effect can lead to large spin-orbit torques of the current.[11,12] Furthermore, basic demonstrations of shift registers have appeared[13] using PMA materials showing their prospect for devices.

The narrow Bloch DWs are, however, very sensitive to local variations in the magnetic and structural properties leading to strong DW pinning.[16] This has lead to many studies concentrating on the depinning of a DW from (intentional) pinning sites. In the case of DW motion the pinning leads to a so-called creep motion of the DW at low drive fields and/or currents.[14] Therefore, a major challenge lies in the control of the intrinsic and extrinsic DW pinning site density and/or strength. In a former study on homogenous films we showed that by doping cobalt with boron, a significant decrease in DW pinning strength was obtained.[15] In this letter we study the DW velocity by a full electrical-transport measurement technique in 900 nm wide strips of Si/SiO_2//Pt(4 nm)/FM(0.6 nm)/Pt(2 nm), where FM stands for ferromagnetic Co or $Co_{68}B_{32}$. We have chosen for 32 at. % boron as this gave the lowest DW pinning in a former study.[15] As expected, we observe a significant increase in DW velocity in the patterned strips indicating that a huge enhancement in DW motion is obtained simply by intrinsically using boron doped cobalt. This is a very promising alternative approach to reduce (intrinsic) pinning and relaxes the need for more advanced patterning techniques that would lead to a reduction in defects such as edge roughness. Furthermore, a reduced DW pinning strength will reduce the critical current density needed for current-induced DW motion and improve the reliability of DW based devices.[13] Finally, we have investigated the morphology of the $Co_{68}B_{32}$ films with high-resolution transmission electron microscopy (HRTEM) to find the origin of the reduced DW pinning.

The devices are prepared by direct sputtering from Pt, Co, and $Co_{68}B_{32}$ targets, electron beam lithography, and ion beam milling. In Fig. 1 we show a scanning electron micrograph (SEM) of the devices including the electrical connections. The device consists of four components labeled (1)–(4). The magnetic strip (1) acts as the DW conduit and is contacted by two large Pt pads (2) at the outer edges, which are used to inject an ac current into the strip by the current source. A passing DW in the strip is detected using the anomalous Hall effect (AHE); three 1 μm wide 10 nm thick Pt Hall probe contacts (3) are patterned on top of the strip, which are each differentially connected to a lock in amplifier (LIA). The Hall probes are spaced 20 μm apart. A DW can be injected into the strip by the Oersted field of a large current pulse passed through the pulse line (Pt, 100 nm thick, 1 μm wide) on top of the magnetic strip (4) using the pulse

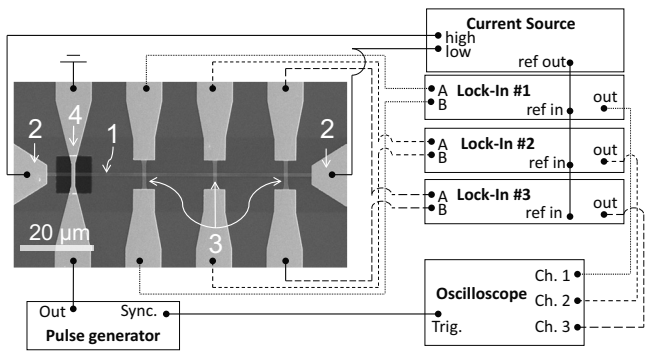

FIG. 1. SEM of used devices including the electrical measurement layout. The 900 nm wide magnetic strip (1) is connected (2) to an ac/dc current source (Keithley 6221). The pulse line (4) is connected to the output of a pulse generator (Agilent 33250A) on one side and grounded on the other. The three Hall probes (3) are differentially connected to individual LIAs (SR830) that lock in to the reference frequency of the ac current source. The output of the lock-ins are connected to an oscilloscope (Agilent DSO80640B), where the data acquisition is triggered by the pulse generator.

a)Electronic mail: r.lavrijsen@tue.nl.

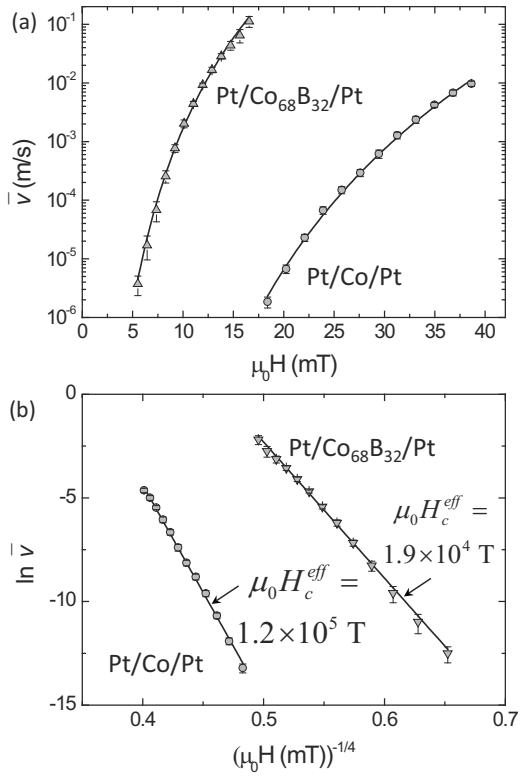

FIG. 2. (a) Average DW velocity vs applied field for patterned 900 nm wide strips of Pt(4 nm)/FM(0.6 nm)/Pt(2 nm) with FM=Co or $Co_{68}B_{32}$. (b) $\ln(v)$ vs $(\mu_0 H)^{-1/4}$ for the same data as presented in (a). The solid lines are a fit to Eq. (1) with the corresponding values of $\mu_0 H_c^{\text{eff}}$ shown in (b).

generator. This pulse line is electrically isolated from the magnetic strip by a 20 nm thick SiO_2 layer (the dark square in the SEM image). Finally, the output of the lock-ins are connected to an oscilloscope, where the data acquisition is triggered by the pulse generator. This allows for synchronized time-resolved measurements of the AHE voltage at the Hall probes, hence, the detection of a DW passing through the magnetic strip.

All the measurements are performed in a cryostat, where we actively control the temperature to $T=300\pm1$ K. A DW passing through the strip is detected by a change of the AHE voltage. To minimize pinning of DWs at the detection points we have patterned the Pt contacts on top of the strip instead of using fully magnetic Hall crosses. In this way a propagating DW will find a constant magnetic strip geometry as it propagates along the strip. To measure the AHE signal we use lock in detection; typically a 100 μA peak-to-peak ac current (10 kHz) is inserted into the magnetic strip. To measure the DW velocity we start with saturating the magnetization of the whole strip, we then set the drive field (below the coercive field of the strip) and use the pulse line ($\sim$45 mA, 500 ns) to insert a DW into the wire. The injected DW will directly propagate through the strip due to the drive field. The propagating DW is detected at the Hall probes and the output signal of the LIA's is recorded by an oscilloscope. We calculate the DW velocity by dividing the distance between two probes by the time it takes a DW to exit one Hall probe and enter the next.

In Fig. 2(a) we show the DW velocity as a function of the applied drive field for Co and $Co_{68}B_{32}$. Every point is the average of 20 measurements and the error bars indicate the standard deviation. All data shown in Fig. 2 are obtained on devices made in the same batch; the measured DW velocity reproduces within 10% between four identical devices. The DW velocities we measure here are in the so-called creep regime.[14,16,17] In the creep regime the DW can be seen as an elastic interface that is thermally activated creeping over local pinning sites, and is described by the following relation:

$$v(H) = v_0 \exp\left[-\left(\frac{H_{dep}}{H}\right)^{\mu}\left(\frac{U_c}{k_B T}\right)\right], \tag{1}$$

where H_{dep} is the critical field below which the creep regime occurs, U_c is the pinning potential, v_0 is a velocity scaling prefactor, k_B is the Boltzmann constant, T is the temperature, and μ is a dynamic exponent. The exponent is shown to depend on the dimensionality and the degrees of freedom of the interface that is under study. The dynamic exponent in this case is equal to 1/4, shown experimentally and theoretically.[14,18] Hence, when the natural logarithm of the velocity is plotted versus $(\mu_0 H)^{-1/4}$ a linear behavior is expected. This is shown in Fig. 2(b), where the same data is plotted as $\ln(v)$ versus $(\mu_0 H)^{-1/4}$. The solid lines in Figs. 2(a) and 2(b) are a fit to the data using Eq. (1). The good agreement of the fits to the data indicates that the motion in the studied velocity range are indeed all in the creep regime. To quantitatively describe the pinning strength we can use an effective critical field defined as $\mu_0 H_c^{\text{eff}} = [U_c/(k_B T)]^4 \mu_0 H_c$ [slope of the data in Fig. 2(b)] reflecting the strength of the pinning potential.[19,20] This gives for Co and $Co_{68}B_{32}$ $\mu_0 H_c^{\text{eff}} = 1.2\times10^5$ T and 1.9×10^4 T, respectively. This shows that by simply doping the Co with boron a factor 6 to 7 reduction in $\mu_0 H_c^{\text{eff}}$ is obtained. In comparison, Cayssol *et al.*[19] find $\mu_0 H_c^{\text{eff}} = 1.15\times10^5$ T for 1 μm wide strips of epitaxially (molecular beam epitaxy) grown AlO_x//Pt(4.5 nm)/Co(0.45 nm)/Pt(3.4 nm). Although this value is surprisingly close to H_c^{eff} in our Co strip, the comparison is rather crude due to the different growth technique and Co layer thickness used in their study. Furthermore, Cayssol *et al.* showed an inverse linear scaling of $\mu_0 H_c^{\text{eff}}$ with the width w of the strips indicating that the edge roughness induces strong DW pinning. Indeed we find $\mu_0 H_c^{\text{eff}} = 2.1\times10^3$ T for a homogenous (nonpatterned) film of Si//Pt(4 nm)/Co(0.6 nm)/Pt(2 nm), similar to Metaxas *et al.*[16] This low value of $\mu_0 H_c^{\text{eff}}$ shows that the edge-roughness-induced pinning in patterned strips dominates the total pinning strength. A further reduction in the pinning strength is therefore conceivable by using boron doped Co together with improved pattering tools to reduce edge roughness, which we intend to address in future studies. We conclude that boron doped Co enhances the field-driven DW creep velocity by a factor 6 to 7 compared to pure Co, showing its excellent potential for DW-motion based experiments and devices with a PMA.

In a former publication we attributed the reduced pinning in $Co_{68}B_{32}$ to a more amorphous growth of the $Co_{68}B_{32}$ layer leading to less grain boundaries, where DWs get pinned.[15] To investigate the growth of the sputtered $Co_{68}B_{32}$ films we performed HRTEM. For this purpose, cross-section TEM lamellas have been fabricated in a dual-beam (electron and ion beam) system. Final thinning of the lamella has been done by operating the ion column at 5 keV to reduce amorphization of the layers induced by surface beam damage. In Fig. 3 we show a HRTEM image of the SiO_2//Pt(4 nm)/$Co_{68}B_{32}$(0.6 nm)/Pt(2 nm) film, where

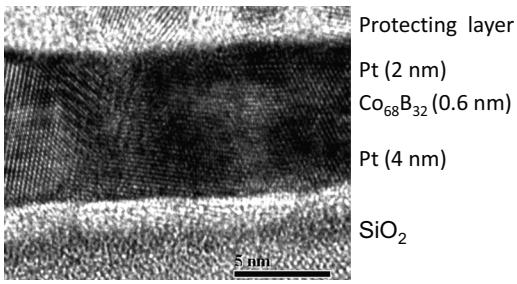

FIG. 3. TEM image of a $SiO_2//Pt(4\ nm)/Co_{68}B_{32}(0.6\ nm)/Pt(2\ nm)$ film. In the image a clear polycrystalline textured film is observed.

on top of the stack a protecting layer has been deposited to protect the lamella. The image shows a highly textured polycrystalline film with a continuation in lattice fringes across all three layers indicating a crystalline growth of the upper two layers on the lower Pt layer. Fourier analysis of individual 5–10 nm wide crystals within the HRTEM image indicates that the polycrystalline film is textured, the texture being a mixture of ⟨111⟩ and ⟨011⟩ components. On comparing this result with pure Co films, we cannot discern a difference in the morphology between the Co or CoB films and hence, we speculate the lowered DW pinning to have a different origin. Alternatively, a decreased DW pinning could be induced by a reduction in the amount of grain boundaries (larger lateral crystals) in the CoB film. It is, however, difficult from these HRTEM images to get an estimate of the lateral grain sizes, and further HRTEM investigation of similar films grown on transparent membranes would be a next step in this analysis.

Another reason for the reduced DW pinning in the CoB samples might be an increased DW width $\Delta = \sqrt{A/K_{\text{eff}}}$, where K_{eff} is the effective PMA and A the exchange stiffness. A wider DW is less sensitive to sharp grain boundaries effectively decreasing the DW pinning strength as also seen in the wide anisotropy boundary steps in focused-ion-beam irradiated films.[10] We estimate Δ to be $\approx$6 nm for Pt/Co/Pt and $\approx$7 nm for $Pt/Co_{68}B_{32}/Pt$ films, where we have used $K_{\text{eff}} = 0.45\ MJ/m^3$ for Pt/Co/Pt and $0.32\ MJ/m^3$ for $Pt/Co_{68}B_{32}/Pt$ as determined from magnetometry measurements and $A = 16\ pJ/m$ as determined by Metaxas *et al.*[16] Please note that we might overestimate Δ in the $Co_{68}B_{32}$ films since a reduced coordination number between the magnetic cobalt atoms in the boron doped film could, in a naive picture of exchange interactions, lead to an effectively lower A. Given these quantitative uncertainties in the relevant parameters for DW motion, we are not able to draw pertinent conclusions on the origin of the significantly suppressed pinning strength for CoB strips. A more systematic study for variable boron composition might shed some light on this issue, including the use of ternary alloys of CoFeB. In the latter case, however, we have observed domain-nucleation dominated magnetization reversal which increased with Fe content. As this is detrimental for DW-motion based studies and devices we do not expect the use of Pt/CoFeB/Pt to be a promising route for further investigation.

In this letter we show that the DW velocity in patterned 900 nm wide $Pt/Co_{68}B_{32}/Pt$ strips is strongly increased compared to identically prepared Pt/Co/Pt strips. This is quantified using the creep scaling law and compared to reports in literature, showing that the boron doped Co shows a strongly decreased DW pinning strength even in patterned films. Furthermore, we investigate the morphology using HRTEM which shows a textured polycrystalline Pt/CoB/Pt film. We foresee that the observed reduced DW pinning in Pt/CoB/Pt films will greatly facilitate the study of field and current driven DW motion.

We thank NanoNed, a Dutch nanotechnology program of the Ministry of Economic Affairs.

[1]S. S. P. Parkin, M. Hayashi, and L. Thomas, Science **320**, 190 (2008).
[2]D. Allwood, G. Xiong, C. Faulkner, D. Atkinson, D. Petit, and R. Cowburn, Science **309**, 1688 (2005).
[3]G. Tatara and H. Kohno, Phys. Rev. Lett. **92**, 086601 (2004).
[4]J. Xiao, A. Zangwill, and M. Stiles, Phys. Rev. B **73**, 054428 (2006).
[5]T. Koyama, G. Yamada, H. Tanigawa, S. Kasai, N. Ohshima, S. Fukami, N. Ishiwata, Y. Nakatani, and T. Ono, Appl. Phys. Express **1**, 101303 (2008).
[6]C. Burrowes, A. Mihai, D. Ravelosona, J.-V. Kim, C. Chappert, L. Vila, A. Marty, Y. Samson, F. Garcia-Sanchez, L. Buda-Prejbeanu, I. Tudosa, E. E. Fullerton, and J.-P. Attané, Nat. Phys. **6**, 17 (2010).
[7]T. A. Moore, I. M. Miron, G. Gaudin, G. Serret, S. Auffret, B. Rodmacq, A. Schuhl, S. Pizzini, J. Vogel, and M. Bonfim, Appl. Phys. Lett. **93**, 262504 (2008).
[8]T. A. Moore, I. M. Miron, G. Gaudin, G. Serret, S. Auffret, B. Rodmacq, A. Schuhl, S. Pizzini, J. Vogel, and M. Bonfim, Appl. Phys. Lett. **95**, 179902 (2009).
[9]R. Lavrijsen, J. H. Franken, J. T. Kohlhepp, H. J. M. Swagten, and B. Koopmans, Appl. Phys. Lett. **96**, 222502 (2010).
[10]J. H. Franken, M. Hoeijmakers, R. Lavrijsen, J. T. Kohlhepp, H. J. M. Swagten, and B. Koopmans, J. Appl. Phys. **109**, 07D504 (2011).
[11]I. M. Miron, P. J. Zermatten, G. Gaudin, S. Auffret, B. Rodmacq, and A. Schuhl, Phys. Rev. Lett. **102**, 137202 (2009).
[12]I. M. Miron, G. Gaudin, S. Auffret, B. Rodmacq, A. Schuhl, S. Pizzini, J. Vogel, and P. Gambarella, Nature Mater. **9**, 230 (2010).
[13]K.-J. Kim, J.-C. Lee, J.-Y. Sang, G.-H. Gim, K.-S. Lee, S.-B. Choe, and K.-H. Shin, Appl. Phys. Express **3**, 083001 (2010).
[14]S. Lemerle, J. Ferre, C. Chappert, V. Mathet, T. Giamarchi, and P. Le Doussal, Phys. Rev. Lett. **80**, 849 (1998).
[15]R. Lavrijsen, G. Malinowski, J. Franken, J. Kohlhepp, H. Swagten, B. Koopmans, M. Czapkiewicz, and T. Stobiecki, Appl. Phys. Lett. **96**, 022501 (2010).
[16]P. J. Metaxas, J. P. Jamet, A. Mougin, M. Cormier, J. Ferre, V. Baltz, B. Rodmacq, B. Dieny, and R. L. Stamps, Phys. Rev. Lett. **99**, 217208 (2007).
[17]P. Chauve, T. Giamarchi, and P. Le Doussal, Phys. Rev. B **62**, 6241 (2000).
[18]G. Blatter, M. Feiglman, V. Geshkenbein, A. Larkin, and V. Vinokur, Rev. Mod. Phys. **66**, 1125 (1994).
[19]F. Cayssol, D. Ravelosona, C. Chappert, J. Ferré, and J. P. Jamet, Phys. Rev. Lett. **92**, 107202 (2004).
[20]L. S. E. Alvarez, K.-Y. Wang, and C. H. Marrows, J. Magn. Magn. Mater. **322**, 2529 (2010).